Analysis of Roll Rotation Mechanism of a Butterfly for Development of a Small Flapping Robot

Masahiro SHINDO[*1], Taro FUJIKAWA[*2], and Koki KIKUCHI[*3]

*1, 3 Department of Advanced Robotics, Chiba Institute of Technology
2-17-1 Tsudanuma, Narashino-shi, Chiba 275-0016, JAPAN
s1376014WE@s.chibakoudai.jp

*2 Department of Robotics and Mechatronics, Tokyo Denki University
5 Senju Asahi-cho, Adachi-ku, Tokyo 120-8551, JAPAN
fujikawa@fr.dendai.ac.jp

Abstract

In this paper, we examine the attitude recovering mechanism of a butterfly by focusing on roll rotation during flight and by developing a fluid solver which analyzes the air flow around the wing using a 3D high speed camera system. Micro aerial vehicles (MAVs) mimicking the flight mechanisms of insects have been developed in recent years. These robots are just a few centimeters in length and have sub-gram weight. However, the attitude and motion controls for such robots have not yet been achieved. The reason for this is that the generation mechanisms of lift and angular moment are still unclear. We clarify the attitude control mechanism of a butterfly by focusing on the pitch and roll rotations. Here we visualized the airflow around a butterfly by computational fluid dynamics which used 3D flight data calculated from 3D high speed camera images as boundary conditions. The results of the analysis showed that the pressure distributions on the wings were different for pitch and roll rotations. In a pitch rotation maneuver, the butterfly changed its pitch angle most significantly. In this case, the differential pressure was concentrated at the fore wings. The maximal reaction force on both sides of the wing and the average angular moment about the pitch axis were 200mN and -32 μNm , respectively. The average rotational moment about the roll axis was 236 μNm . In a roll rotation maneuver, the butterfly changed its roll angle most significantly. In this case, the differential pressure was distributed across the whole wing including the hind wing. The maximum reaction forces on the left and right wings and the average angular moment about the roll axis were 400mN, 220mN, and -282 μNm , respectively. These results show that a butterfly controls its attitude by changing the distribution of the differential pressure during flight.

Keywords: CFD, MAV, butterfly, flapping flight, roll rotation, attitude control

1 Introduction

Birds and insects flap to achieve flight and can perform wonderful aerial feats such as vertical takeoff and landing, snap turns, and hovering. They gain high maneuverability by utilizing the vortices around the wings. A butterfly is a suitable model on which to base autonomous micro aerial vehicles (MAV), due to its sub-gram weight, low flapping frequency and a few degrees of freedom compared to other flying insects. To develop a small flapping robot, many studies on the flight mechanism of butterflies have been carried out. Takahashi *et al.* have developed a micro strain sensor using micro electronic mechanical systems (MEMS) and measured pressure by mounting it on the wings [1]. The result of measurement showed that the differential pressure on the fore wings was dominant over the pressure on the hind wings. However, in this experiment, the butterfly flew while pulling a signal wire because the sensor was physically connected to an external circuit board. Therefore, it is possible that the flight behavior was different to that of an untethered butterfly. Fuchiwaki *et al.* have visualized vortices around two kinds of butterfly using particle image velocimetry (PIV) [2]. The results show that a vortex ring is formed at the beginning of the down stroke and passes over the body with growing vorticity and flow speed regardless of the type of a butterfly. The PIV method is able to analyze the air flow in an arbitrary plane in space; however, flapping is a complex 3D action which requires the 3D visualization of vortices.

We clarify the attitude recovering mechanism of a butterfly by analyzing an untethered butterfly and visualizing the pressure and vortices. We photograph the flapping behavior using a 3D high speed camera system. The 3D data from different points on the butterfly wings are obtained from all three directions. The attitude (roll, pitch, and yaw angles) and flapping angle are determined by using these points. These points and velocities are also used as the boundary conditions for computational fluid dynamics (CFD). By reproducing the actual behavior of a butterfly in a computer, the airflow around the measured points can be deduced. Based on this numerical procedure, the magnitude and distribution of pressure and the behavior of the vortices can be visualized. Accordingly, the lift and drag forces on the butterfly are calculated by considering the pressure over the whole wing. This study clarifies the roll rotation mechanism of a butterfly by determining the reaction force exerted by the left and right wings and the angular moments during flight.

Copyright © 2014, The Organizing Committee of the ICDES 2014

2 Photography of flight behavior

2.1 Analysis of the images

In this study, we photographed the free flight behavior of *Papilio xuthus* using a 3D high speed camera system (**Fig. 1**). The camera coordinate system has three axes parallel to the camera directions and its origin is fixed at the takeoff point of the butterfly. All cameras are located 1,500mm from the roost. **Table 1** shows the photography parameters. The captured space is $250\times250\times250\text{mm}^3$. The positions of the cameras are identified by calibration using a target, and then the coordinates of the measured points are calculated using epipolar geometry.

Figure 2 shows the measured points of the butterfly. The body is divided into three parts: head, thorax, and abdomen (B_1-B_4 in **Fig. 2**). The measurements of the wings are carried out along the edges since the opaque wings occlude points on the surfaces frequently during flight (L_1-L_9 and R_1-R_9 in **Fig. 2**).

2.2 Definitions of the parameters

To determine the attitude and flight parameters of a butterfly, we define the butterfly coordinate system Σ_B (**Fig. 3**). The X_B axis is the vector from B_1 to B_3. The Z_B axis is the vector product of the X_B axis and the body-span vector from L_1 to R_1. The Y_B axis is the vector product of Z_B and X_B.

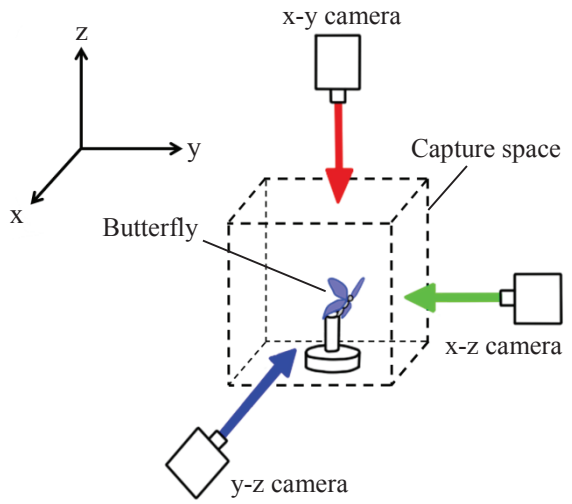

Fig. 1 Camera arrangement

Table 1 Camera configuration

Frame rate	1000 frame/sec
Image resolution	1280× 1024 pixels
Shutter speed	1/5000 sec

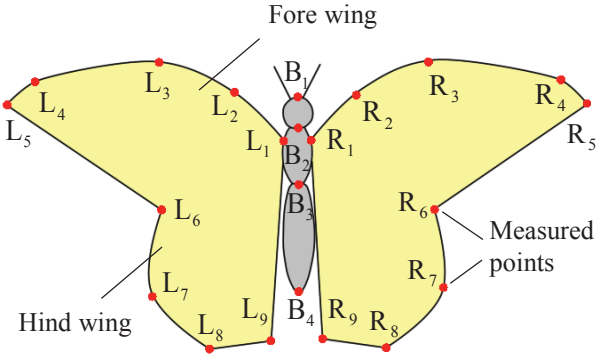

Fig. 2 Measured points of body and wings

The attitude of the butterfly is shown in **Fig. 3**, in which the roll, pitch, and yaw angles are denoted by Φ, θ, and ψ, respectively. Here, we define horizontal and vertical body planes that have Z_B and X_B as normal vectors. The roll, pitch, and yaw angles are defined as follows: Φ is the angle between the horizontal body plane and the Y axis, θ is the angle between the horizontal body plane and the X axis, and ψ is the angle between the vertical body plane and the Y axis.

The flight parameters describing the state of the butterfly are chosen as follows: The angle between the horizontal body plane and the normal vector of the fore wing is defined as the flapping angle. The flapping cycle is divided into two phases, up and down strokes. We also define the lead-lag angle as a parameter which describes the wing state. The lead-lag motion of a butterfly controls not only the pressure center on the wings but also the wing area by overlapping the fore and hind wings [3-5]. This motion is parameterized by the angle between the vertical body plane and the vector from the root to the tip of the wing. The parameter describing the state of the abdomen is as follows: A butterfly swings its abdomen horizontally and vertically as well as flapping. The vertical abdomen angle is defined as the angle between the horizontal body plane and the abdomen vector from B_3 to B_4. The horizontal abdomen angle is the angle between the body and the abdomen vectors.

3 Computational fluid dynamics

3.1 Boundary conditions around a butterfly

In this study, we analyzed the flow field around a real

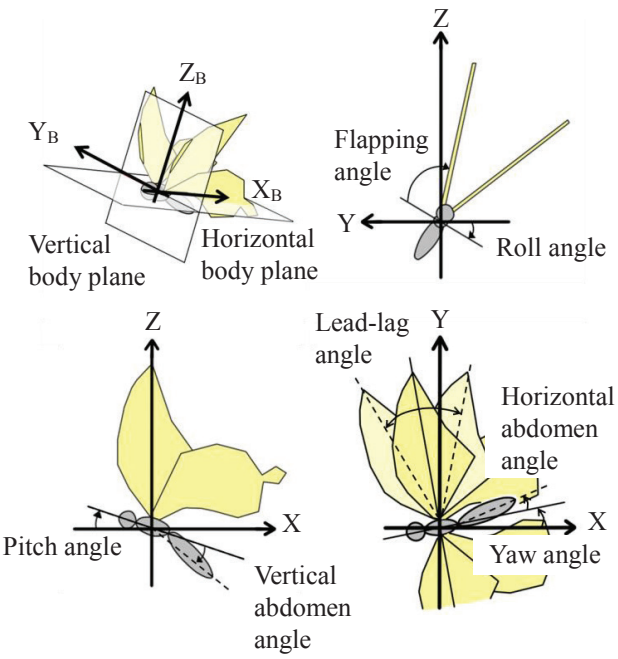

Fig. 3 Definitions of the axes, planes, and angles of the butterfly

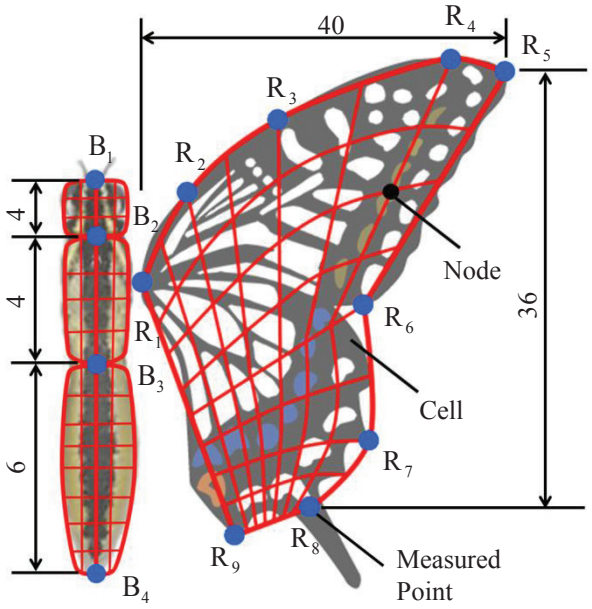

Fig. 4 Meshing of a butterfly for CFD

butterfly flying in the imaging space. Using the measured points and velocities defined in the previous section as the mesh boundaries, the behavior of real vortices can be visualized. The wing and body are divided into meshes bounded by the measured points (**Fig. 4**). The leading edges of the fore wings (L_1-L_5 and R_1-R_5) and the side edges of the hind wings (L_6-L_8 and R_6-R_8) are approximated to match a butterfly wing shape using 3rd order spline interpolation. The body and other wing sections are divided linearly. To simplify the calculation, our simulation considers the fore and hind wings as one. The body of the butterfly model is composed of three parts, head, thorax, and abdomen. These parts are cylindrical and their axes are the lines which join the measured points. The coordinates of the butterfly are obtained by image processing every millisecond using a 1000 frame per second camera. To improve calculation accuracy, we further divided these data intervals into 0.01 millisecond periods through spline interpolation. In the interpolation process, the acceleration at both edges of the approximate curve is assumed to be zero. The approximate curve is continuous up to 2nd order.

3.2 Governing equations of flow

The numerical solver in this study analyzes the air flow caused by the flapping motion of the butterfly using the measured points and velocities as the boundary conditions. The governing equations for CFD are the continuity equation and the Navier-Stokes equation. The flow is considered to be 3D, incompressible, and unsteady. In Equ. (1), U, ρ, P, and μ are the mean velocity vector of flow, density, pressure, and the coefficient of viscosity, respectively.

$$\begin{cases} \nabla \cdot U = 0 \\ \dfrac{\partial U}{\partial t} + (U \cdot \nabla)U = -\dfrac{1}{\rho}\nabla P + \dfrac{\mu}{\rho}\nabla^2 U \end{cases} \quad (1)$$

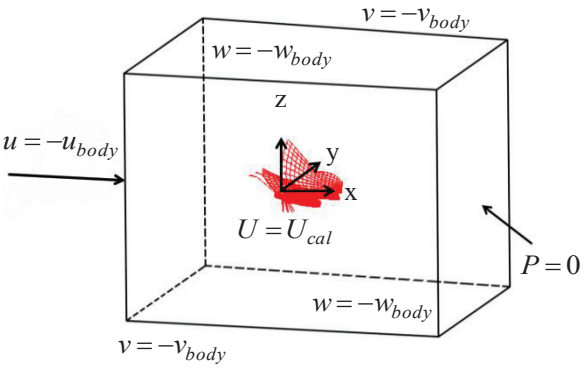

Fig. 5 Calculation space and boundary conditions

Finite element method (FEM) was used for the calculation scheme. This method is stable and maintains high accuracy with large mesh deformation. The calculation space mesh tends to deform because the flapping range of a butterfly is far wider than that of other insects, at almost 180deg. Therefore, we adopt an arbitrary Lagrangian-Eulerian (ALE) method for the deformation and motion of the calculation space and butterfly meshes. The calculation of flow is stabilized using the stream-upwind/Petrov-Galerkin (SUPG) method. Dividing the Navier-Stokes equation into two terms using a simplified marker and cell method (SMAC) method allows the explicit and implicit calculations of velocity and pressure, respectively.

The size of the calculation space is $130 \times 100 \times 100\text{cm}^3$ and the number of nodes for FEM is $94 \times 108 \times 75$. **Figure 5** shows the boundary conditions of the space. Here, u_{body}, v_{body}, w_{body}, u_{cal}, v_{cal}, and w_{cal} denote the velocities of the butterfly and the wall. The origin of the coordinate system of the calculation space is fixed at the initial position of the thorax and the X axis points in the opposite direction to the butterfly's movement.

4 Fluid analysis around the butterfly

We photographed two kinds of maneuvers in which the butterfly rotated around different axes, to clarify the butterfly's rotation mechanisms. Section 4.1 describes a pitch rotation which is a typical maneuver for a butterfly. Section 4.2 describes a roll rotation and clarifies the attitude recovering mechanism for rotating from a rolled state to a horizontal state.

4.1 Flow field of pitch rotation maneuver

In this section, we describe the typical pitch rotation maneuver. The initial attitude of the butterfly was Φ =1.5deg, θ=23.4deg, and ψ=-2.8deg. **Figure 6** shows the transitions of the flapping, pitch, and roll angles. It can be seen that the pitch angle increased simultaneously with the downstroke. The wing motion changed from the downstroke to the upstroke at a flapping angle of -70deg. The pitch angle continued to increase for 10ms after the stroke reversal. The reaction force on the wing provided the thrust since the stroke was in the positive X direction. In the upstroke phase from 31ms to 81ms, the butterfly flew forward with decreasing pitch angle. The down stroke started again at

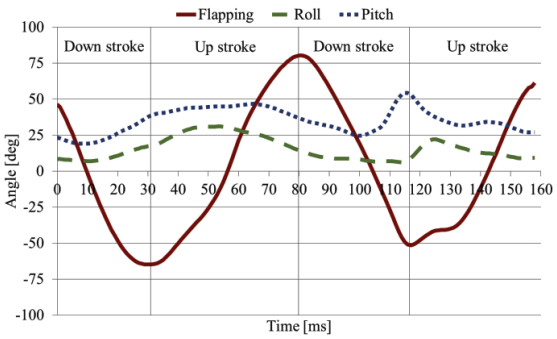

Fig. 6 Time history of the angles: pitch rotation maneuver

a flapping angle of 80deg. As well as the first stroke, the pitch angle transitions lagged behind the change in stroke by 10ms. The roll angle was almost unchanged throughout the two flapping cycles. The maximum variation was 25deg at a flapping angle of -10deg during a first upstroke (**Fig.6A**).

Figure 7 shows the streamlines around the wings caused by the flapping motion. The streamlines are colored according to the flow speed, where the red lines are faster and blue lines are slower. The leading-edge vortices (LEV) and wing tip vortices (WTV) which were present on the upper surface of the wing were generated during the down stroke. These vortices decrease pressure causing the differential pressure between the top and bottom surfaces of the wing. Dickinson *et al.* have reported the lift generation mechanisms [6], which are as follows. Rotational circulation means that the rotation of the wing at the time of the stroke reversal generates an upward force. The wake capture mechanism explains the increase in aerodynamic force during the stroke reversal. **Figure 8** shows the twist angle of the left and right wings during two flapping cycles. It shows that the twist angle changed at the time of the stroke reversal. We think that the lift force was increased by rotational circulation at that time [6]. The axes of the vortices are parallel to the wing surface.

Figure 9 shows the constant pressure surfaces on the wings as stroboscopic images. The red and blue surfaces show positive and negative pressures of 0.8Pa and -0.8Pa, respectively. The pressure is positive on the upper side and negative underneath during the down stroke. The butterfly rose with increasing pitch angle due to the differential pressure that concentrated near the leading-edge of the fore wings. The pressure is positive underneath the wings and negative on the upper side during the upstroke. Similarly to the down stroke, the butterfly flew forward with decreasing pitch angle due to the differential pressure that concentrated near the leading-edge of the fore wings.

Figure 10 shows the time history of the reaction force on the left and right wings. During the pitch rotation maneuver, the reaction forces of the left and right wings were changed in the similar tendency. The force on the right wing exceeded that on the left wing during the first down stroke. This continued until the upstroke at 46ms, at which time the roll angle also increased. From the start of the second flapping cycle,

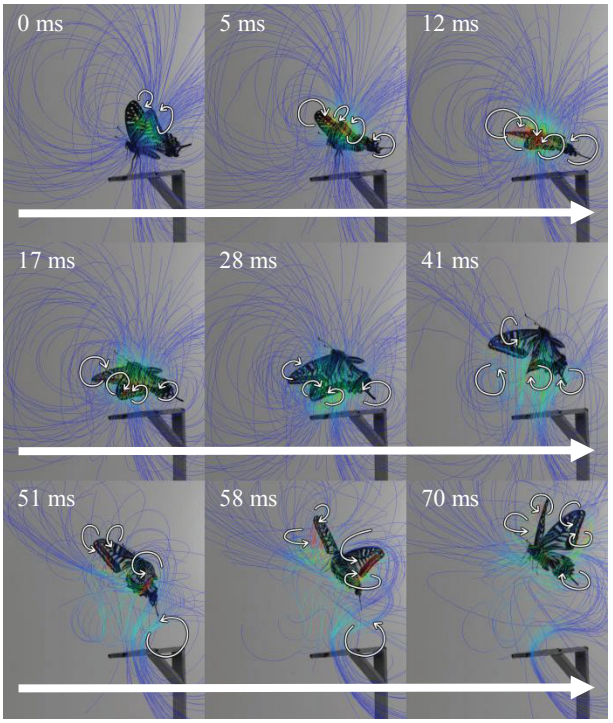

Fig. 7 Stroboscopic images of streamlines: pitch rotation maneuver

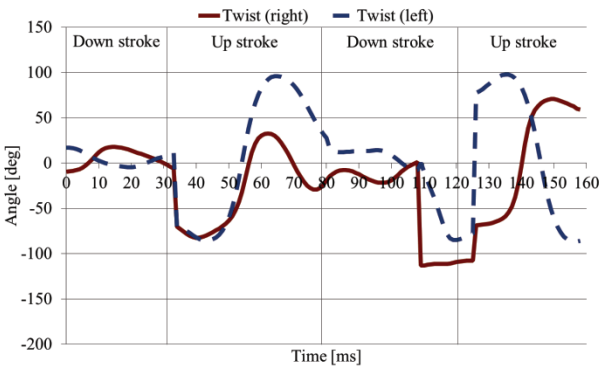

Fig. 8 Time history of twist angles: pitch rotation maneuver

the reaction forces on the left and right wings were the same and the roll angle of the butterfly did not change.

4.2 Flow field of roll rotation maneuver

This section describes the mechanism for rotating from a rolled state to a horizontal state. The initial attitude of the butterfly was Φ=-58.0deg, θ=52.1deg, and ψ=-87.8deg. **Figure 11** shows the transition of the flapping, pitch, and roll angles. Unlike the previous flight pattern, the maximum variation in pitch angle was 25deg. The pitch angle decreased with the down stroke because the butterfly took off from the bottom side of the roost. The roll angle also decreased and the butterfly rotated around the roll axis in the clockwise direction.

The reaction force acted in the negative X direction since the pitch angle was 50deg. The butterfly moved 5mm in the Z direction. The down stroke ended and the upstroke began at a flapping angle of -50deg. The pitch

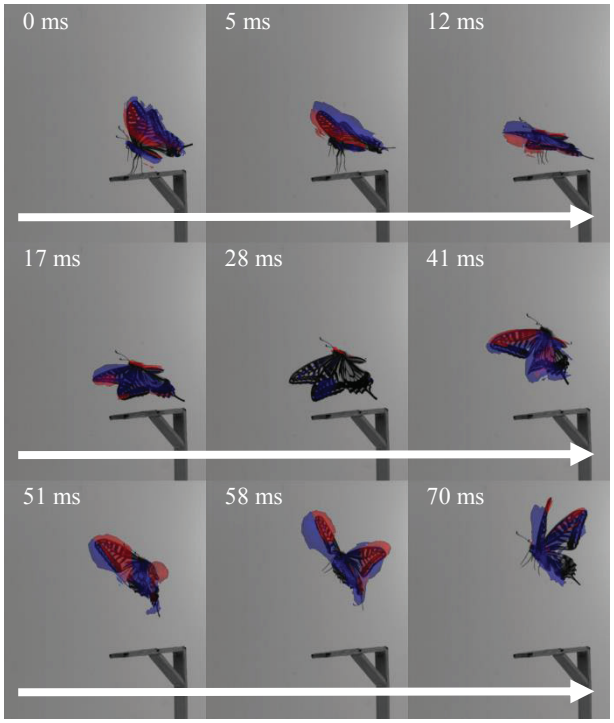

Fig. 9 Stroboscopic images of the constant pressure surface: pitch rotation maneuver

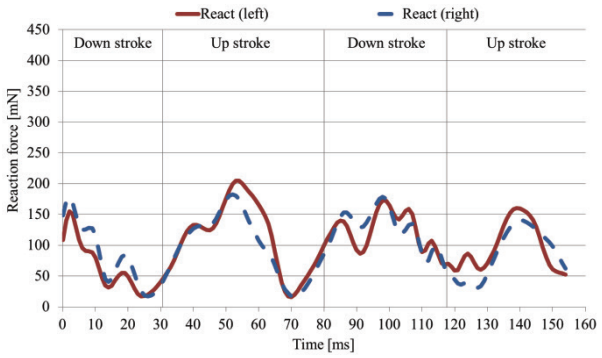

Fig. 10 Time history of the reaction forces: pitch rotation maneuver

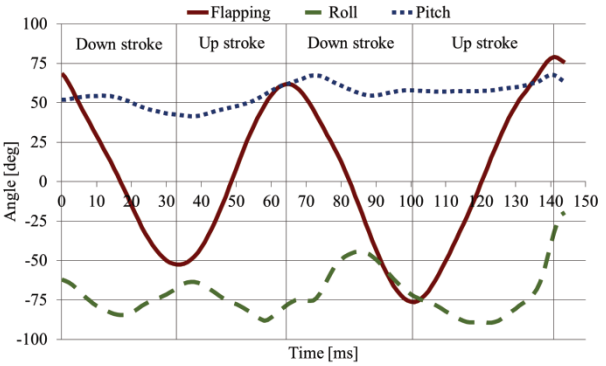

Fig. 11 Time history of the angles: roll rotation maneuver

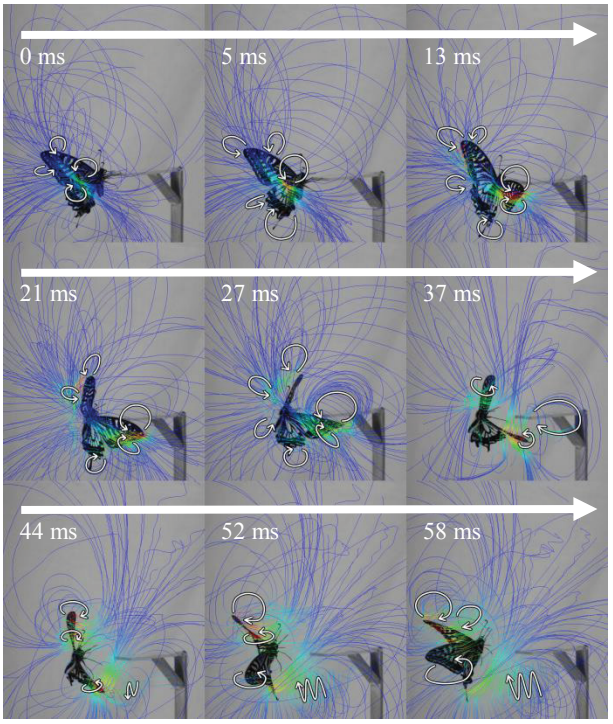

Fig. 12 Stroboscopic images of streamlines: roll rotation maneuver

angle decreased for 10ms at the beginning of the upstroke. After that, it continued to increase until reaching a maximum at a flapping angle of 75deg. On the second down stroke, the flapping motion of the right wing preceded that of the left wing by 5ms. From this point the roll angle started to change. From 65ms, the rotational moment around the roll axis increased over 5ms because the direction of the reaction forces on the right and left wings were different.

Figure 12 shows the streamlines around the wing. The LEVs and WTVs, which were present on the upper surface of the wing, were generated during the down stroke, as in the pitch rotation maneuver. **Figure 13** shows that although the twist angle decreased from the beginning of down stroke, it increased 10ms before the stroke reversal. We conclude that the butterfly, similarly to *Drosophila*, used rotational circulation by advancing the fore wing to the hind wing [6-7]. The behavior of the vortices during the upstroke was different to that in the pitch rotation maneuver. In this case, the axis of the WTVs intersected the wings.

Figure 14 shows the constant pressure surfaces at the same time as those shown in **Fig. 12**. The pressure distribution during the down stroke was similar to that in the pitch rotation maneuver; however, that in the upstroke was different. The differential pressure during the upstroke concentrated near the leading-edges of the fore wings during the pitch rotation. In the roll rotation, however, it extended across the whole wing. The variation in pitch rotation was slight because the magnitudes of the reaction forces on the wings were equal. **Figure 15** shows the time history of the reaction force on the wings. The reaction force on the right wing preceded that on left wing by 5ms when the second down stroke started. The butterfly rotated around the roll axis due to the angular moment generated. During the second down stroke, the maximum force on the right wing was 400mN, while that on the left wing was 220mN. The reaction force on the left wing was also larger than that on the right wing during the second

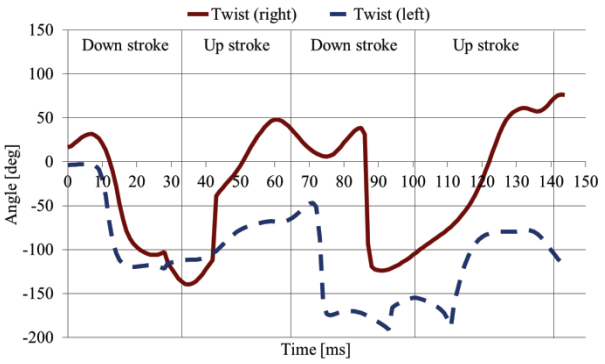

Fig. 13 Time history of twist angles: roll rotation maneuver

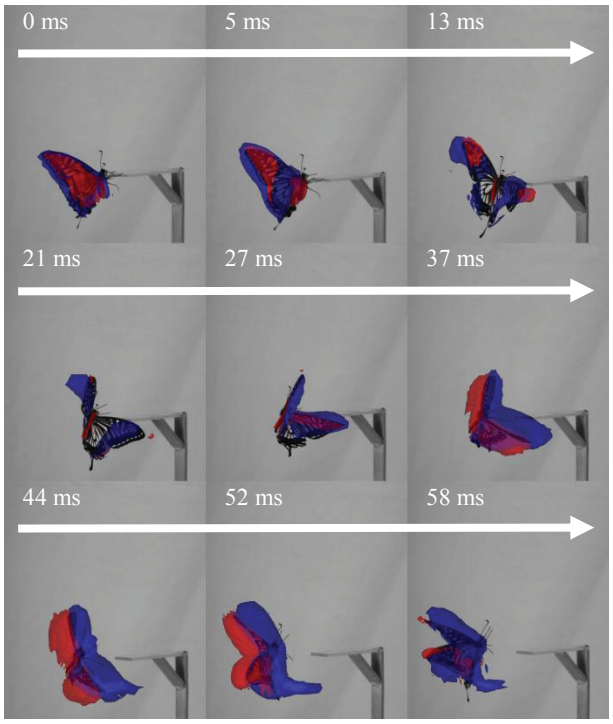

Fig. 14 Stroboscopic images of the constant pressure surface: roll rotation maneuver

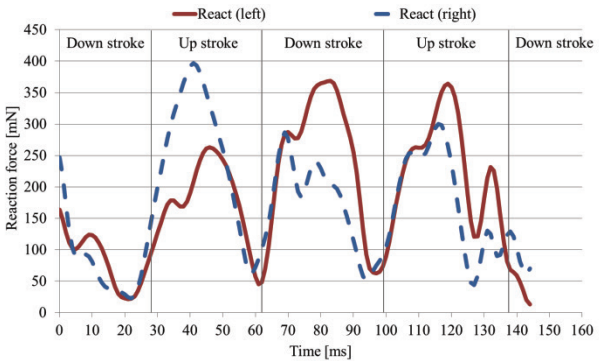

Fig. 15 Time history of the reaction force: roll rotation maneuver

upstroke. The roll attitude of the butterfly, which was initially roll-rotated at -58deg, became approximately horizontal at the start of the third down stroke.

5 Conclusion

In this paper, we analyzed vortices around the wings of a butterfly using CFD and clarified the attitude control mechanism for roll rotation. The results showed that the pressure distribution and behavior of the vortices changed according to the changes in attitude. In the case of a pitch rotation maneuver, the pitch angle changed most significantly and the differential pressure concentrated near the leading edges of the fore wings. The maximum reaction force on both sides of the wing and the average angular moment about the pitch axis were 200mN and -32 μNm, respectively. In the case of a roll rotation maneuver, the roll angle changed most significantly and the differential pressure was distributed across the whole wing. The maximum reaction force on the left wing was 400mN and that on the right wing was 220mN. The differential force generated an angular moment about the roll axis, which was -282 μNm on average during the maneuver. These results show that the butterfly controlled its rotational direction by changing the pressure distribution.

In future work, long-term flight will be analyzed to clarify the attitude stabilization mechanisms.

References

[1] Hidetoshi Takahashi, Kiyoshi Matsumoto, and Isao Shimoyama, “Differential Pressure Measurement of an Insect Wing Using a MEMS Sensor”, International Conference on Complex Medical Engineering, pp.349-352.

[2] Masaki Fuchiwaki, Taichi Kuroki, Kazuhiro Tanaka, and Takahide Tababa, “Dynamic behavior of the vortex ring formed on a butterfly wing”, Experimental in Fluid, 2013, pp.13-24.

[3] Taro Fujikawa, Yoshinori Sato, Tatsuhiko Yamashita, and Koki Kikuchi, “Development of A Lead-Lag Mechanism Using Simple Flexible Links for A Small Butterfly-Style Flapping Robot”, WAC2010 (ICDES2005, MSSP2008, ISIAC2010), 2010, pp.1-6.

[4] Taro Fujikawa, Kazuaki Hirakawa, Shinnosuke Okuma, Takamasa Udagawa, Satoru Nakano, and Koki Kikuchi, “Development of a small flapping robot: Motion analysis during takeoff by numerical simulation and experiment”, Mechanical Systems and Signal Processing Vol.22, 2008, pp.1304-1315.

[5] Takamasa Udagawa, Taro Fujikawa, Xueshan GAO, and Koki Kikuchi, “Development of a Small-Sized Flapping Robot”, JSDE The 1st ICDS, 2005, pp.283-288.

[6] Michael H. Dickinson, Fritz-Olaf Lehmann, and Sanjay P. Sane, “Wing Rotation and the Aerodynamic Basis of Insect Flight”, Science Vol. 284, 1999, pp.1954-1960.

[7] Fritz-Olaf Lehmann1, Sanjay P. Sane, and Michael Dickinson, “The aerodynamic effects of wing-wing interaction in flapping insect wings”, The Journal of Experimental Biology, Vol.208, 2005, pp.3075-3092.

Received on October 30, 2013
Accepted on January 28, 2014